# Multiple modes of instability in a box heated from the side in low-Prandtl-number fluids

D. Henry and H. BenHadid
*Laboratoire de Mécanique des Fluides et d'Acoustique, CNRS/Université de Lyon, Ecole Centrale de Lyon/Université Lyon 1/INSA de Lyon, ECL, 36 avenue Guy de Collongue, 69134 Ecully Cedex, France*

(Received 22 May 2007; accepted 16 July 2007; published online 28 August 2007)

The existence of multiple modes of instability in Rayleigh-Bénard or Marangoni-Bénard situations has been known for many years. This existence is shown for the first time for low-Prandtl-number flows in three-dimensional cavities heated from the side. For such a situation, the study of the flow transitions has long remained a challenge, as these transitions occur in already very intense flows. The study is possible here thanks to performing numerical methods, and the ten first instability modes are determined for a wide range of aspect ratios and Prandtl number values. The most striking feature of our results is the very frequent change of leading mode when aspect ratios or Prandtl number are changed, which indicates different flow structures triggered at the transitions, either steady or oscillatory and breaking some of the symmetries of the problem. © *2007 American Institute of Physics*. [DOI: 10.1063/1.2770514]

Sidewall convection is a heat and mass transfer problem of significance in both fundamental fluid mechanics and engineering applications such as crystal growth.[1] In the case of the flow in a parallelepipedic cavity, the basic flow is a simple unicellular circulation. When the horizontal temperature gradient is increased, however, the flow becomes more complex, undergoes bifurcations, becomes unsteady, and eventually turbulence sets in for large temperature differences.

Our interest is in the first onset of time dependence in such convective flows, with relevance to metallic or semiconductor materials processing. In practical flows, instabilities in the melt phase during crystal growth can be frozen into the solid product and can degrade the performance of semiconductor devices.[2] The melts are good thermal conductors, so that the Prandtl number Pr (the ratio of the viscous to the thermal diffusivity) is small. This will support our choice of small values of Pr ranging from 0 to 0.03. The other important parameters of these situations are the aspect ratios of the cavity (relative dimensions scaled by the dimensional height) and the Grashof number Gr proportional to the applied temperature difference.

Quite a lot of work has been done on the transition to unsteady convection in rectangular cavities in low-Prandtl-number fluids, from the first experimental work of Hurle *et al.*[3] in 1974, to the stability studies assuming one-dimensional parallel flow in an infinitely extended layer,[4,5] the experimental investigations and two-dimensional simulations connected to the numerical benchmark proposed in a GAMM workshop[6] in 1990, and, more recently, new experiments[7] and three-dimensional numerical simulations.[8–10] Nevertheless, no study clearly underlined the different transitions encountered when changing the parameters of the problem.

Our study concerns convection in a three-dimensional parallelepipedic cavity and is focused on the determination of the leading modes involved in the first flow transition for a wide range of aspect ratios and Prandtl number values. For that, close to the threshold, the ten dominant eigenmodes are calculated, among which the leading mode (i.e., the mode that first acquires a positive real part of the eigenvalue) is really the mode of physical relevance as it will drive the transition to new stable flow states. The calculation of several dominant eigenmodes (and not only the leading one), however, is a key point to understand the change of leading mode. For the first time, we are able to show the numerous different modes which determine the structure of the flows at the first transition and how these modes compete when changing the aspect ratios or the Prandtl number. If such a competition between modes was well known in the Rayleigh-Bénard situation (and for example concerns the azimuthal modes in a vertical cylinder), the result is really new for sidewall convection. Finally, we have to mention that this analysis is purely linear, and that only a nonlinear analysis (beyond the scope of this work) can indicate the supercritical or subcritical nature of the bifurcations and the possible existence, in the second case, of new stable solutions well below the bifurcation lines.

The mathematical model consists of a rectangular parallelepiped cavity filled with low-Pr fluids and heated from the side. The cavity has aspect ratios $A_x=L/h$ and $A_y=l/h$, where $L$ is the length of the cavity (along $x$), $h$ its height (along $z$) and $l$ its width (along $y$), as shown schematically in Fig. 1. The vertical endwalls are isothermal and held at different temperatures, i.e., $\bar{T}_h$ at the right hot endwall and $\bar{T}_c$ at the left cold endwall, whereas the sidewalls are adiabatic. The fluid is assumed to be Newtonian with constant physical properties (kinematic viscosity $\nu$, thermal diffusivity $\kappa$, density $\rho$), except that, according to the Boussinesq approximation, the fluid density is considered as temperature dependent in the buoyancy term with a linear law $\rho=\rho_m[1-\beta(\bar{T}-\bar{T}_m)]$,

 

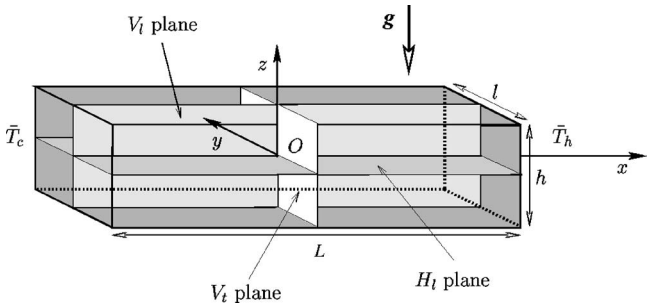


FIG. 1. Geometry of the differentially heated cavity.

where $\beta$ is the thermal expansion coefficient and $\bar{T}_m$ a reference temperature taken as the mean temperature $(\bar{T}_h+\bar{T}_c)/2$. The convective motions are then modeled by the Boussinesq equations coupled to an energy equation. Using $h$, $h^2/\nu$, $\nu/h$, $\rho\nu^2/h^2$, and $\gamma=(\bar{T}_h-\bar{T}_c)/A_x$ as scales for length, time, velocity, pressure, and temperature, respectively, these equations take the following form:

$$\nabla\cdot\boldsymbol{u}=0,$$

$$\partial\boldsymbol{u}/\partial t+(\boldsymbol{u}\cdot\nabla)\boldsymbol{u}=-\nabla p+\nabla^2\boldsymbol{u}+\mathrm{Gr}\,T\boldsymbol{e}_z,$$

$$\partial T/\partial t+(\boldsymbol{u}\cdot\nabla)T=(1/\mathrm{Pr})\nabla^2 T,$$

with boundary conditions given by $\partial T/\partial z=0$ on $z=\pm 1/2$ and $\partial T/\partial y=0$ on $y=\pm A_y/2$, $T=-A_x/2$ on $x=-A_x/2$ and $T=A_x/2$ on $x=A_x/2$, and $\boldsymbol{u}=0$ on all boundaries. The dimensionless variables are the velocity vector $\boldsymbol{u}=(u,v,w)$, the pressure $p$, and the temperature $T=(\bar{T}-\bar{T}_m)/\gamma$, $\boldsymbol{e}_z$ is the unit vector in the vertical direction, and the nondimensional parameters are the Grashof number $(\mathrm{Gr}=\beta g\gamma h^3/\nu^2)$ and the Prandtl number $(\mathrm{Pr}=\nu/\kappa)$.

In the approximation of the model, the steady convective flows obtained at moderate Gr in such a cavity[9] present different symmetries: a reflection symmetry $S_l$ with respect to the longitudinal $V_l$ plane (left-right symmetry) and a $\pi$-rotational symmetry $S_r$ about the transverse $y$ axis. The combination of these two symmetries gives a symmetry $S_c$ with respect to the center point of the cavity $(S_c=S_l\cdot S_r)$. When increasing Gr, steady or oscillatory instabilities will occur, which will usually break some of these symmetries.

The governing equations of the model are solved in the three-dimensional domain using a spectral element method, as described in BenHadid and Henry.[11] The time discretization is carried out using a semi-implicit splitting scheme where the nonlinear terms are first integrated explicitly, the pressure is then solved through a pressure equation enforcing the incompressibility constraint, and the linear terms are finally integrated implicitly. This time integration scheme is used for transient computations with a third-order accurate formulation. However, in this paper, we focus on following steady flow solutions by incrementing Gr, $A_x$, $A_y$, or Pr, and calculating their stability in order to identify the dominant instability modes. The Newton method described by Mamun and Tuckerman[12] and already used in Bergeon *et al.*[13] is used to calculate each steady state solution. The main idea is to solve the linear systems appearing at each Newton step by an iterative solver, and to compute right-hand sides and matrix-vector products corresponding to these linear systems by performing adapted first order time steps of the basic or linearized problem. An advantage of this method is that the Jacobian matrix does not need to be constructed or stored. The GMRES algorithm is used as the iterative solver. The calculation of the ten dominant eigenvalues—those with largest real part—and their corresponding eigenvectors is performed using Arnoldi's method (ARPACK library) by timestepping the linearized equations, as described in Mamun and Tuckerman.[12]

Our results concern various cavities ranging from $A_x=2$ to $A_x=5$ and from $A_y=1$ to $A_y=6$. For all these cavities, the same refined mesh corresponding to $47\times 27\times 49$ points has been chosen. It gives a good precision in any case.

Our study is focused on the determination of the leading instability modes involved in the first flow transitions, for a wide range of aspect ratios and Prandtl numbers. We want to see how these parameter changes can affect the type of flow transition which will be observed. For Pr=0.01 we first changed the longitudinal aspect ratio $A_x$ from 2 to 5 for a cavity with a large transverse extension $(A_y=6)$. For the same value of Pr and $A_x=4$, we widely changed the transverse confinement with $A_y$ varying from 6 to 1. Finally, the effect of the Prandtl number $(0.00001\leq\mathrm{Pr}\leq 0.03)$ was studied for the cavity $A_x=4$ and $A_y=2$ already considered by

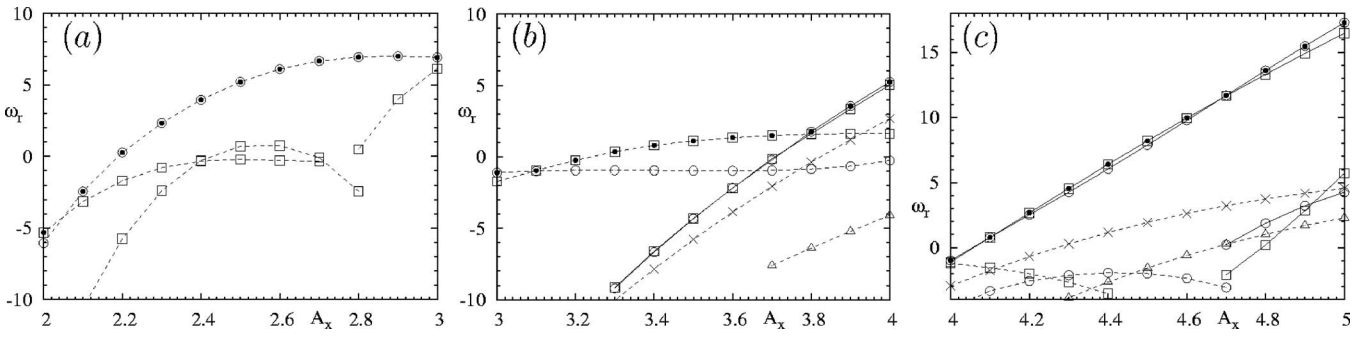


FIG. 2. Real parts $\omega_r$ of the dominant eigenvalues for $2\leq A_x\leq 5$ ($A_y=6$ and Pr=0.01): (a) Gr=34 000 for $2\leq A_x\leq 3$, (b) Gr=23 000 for $3\leq A_x\leq 4$ and (c) Gr=20 000 for $4\leq A_x\leq 5$. Solid curves represent steady modes and dashed curves oscillatory modes. Circles indicate $S_c$ modes, squares $S_l$ modes, triangles $S_r$ modes, and crosses $S$ modes. The black dots indicate the leading mode.

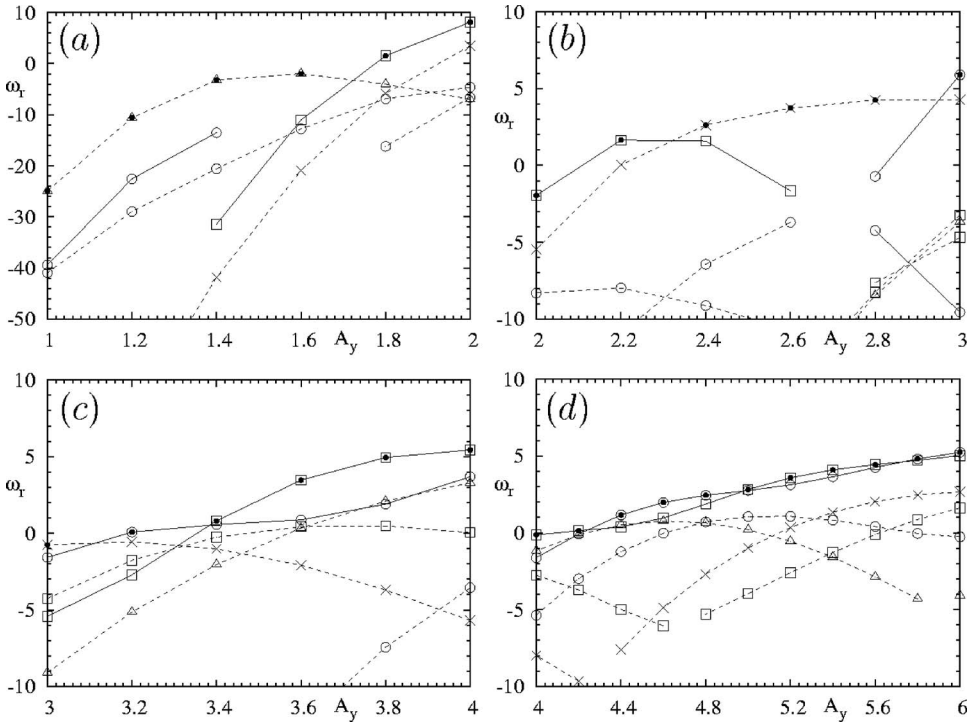


FIG. 3. Real parts $\omega_r$ of the dominant eigenvalues for $1 \leq A_y \leq 6$ ($A_x=4$ and Pr=0.01): (a) Gr=35 000 for $1 \leq A_y \leq 2$, (b) Gr=30 000 for $2 \leq A_y \leq 3$, (c) Gr=26 000 for $3 \leq A_y \leq 4$, and (d) Gr=23 000 for $4 \leq A_y \leq 6$. Solid curves represent steady modes and dashed curves oscillatory modes. Circles indicate $S_c$ modes, squares $S_l$ modes, triangles $S_r$ modes, and crosses $S$ modes. The black dots indicate the leading mode.

Henry and Buffat.[9] The steps used for changing these parameters were 0.1 for $A_x$, 0.2 for $A_y$, and 0.001 for Pr.

The calculations were initiated for $A_x=4$, $A_y=6$, and Pr=0.01. A steady solution corresponding to a unicellular circulation was first obtained by temporal evolution for Gr=20 000. Other steady solutions were then obtained by continuation for increasing values of Gr, and their stability was checked by Arnoldi's method. In this way, the critical threshold for this situation was estimated at about $Gr_c=20\,500$. The leading mode was steady and only kept the central symmetry. It is from this case that we studied the influence of $A_x$ on the flow transitions. The value of Gr was chosen not too far from the critical transitions. Practically, we fixed it to a given value in different ranges of $A_x$: Gr=20 000 for $4 \leq A_x \leq 5$, Gr=23 000 for $3 \leq A_x \leq 4$ and Gr=34 000 for $2 \leq A_x \leq 3$. For all these cases, the steady solution was calculated by continuation from previously obtained solutions and the ten dominant eigenvalues were estimated by Arnoldi's method. The evolution of the real part $\omega_r$ of these eigenvalues is given in Fig. 2. In this figure as in the other figures giving eigenvalues, different symbols are used to characterize the symmetries of the eigenvector associated to the eigenvalue. More precisely, squares are used to indicate eigenvectors with the $S_l$ (left-right) symmetry ($S_l$ modes), circles for eigenvectors with only the $S_c$ (central) symmetry ($S_c$ modes), triangles for eigenvectors with the $S_r$ ($\pi$-rotational) symmetry ($S_r$ modes), and crosses for eigenvectors having kept all the symmetries (which we will call the $S$ symmetries, and the corresponding modes, $S$ modes). Moreover the curves are plotted with a solid line for the steady modes and with a dashed line for the oscillatory modes, and the leading mode (in fact the one which has the strongest $\omega_r$ at the given Gr) is indicated by a black dot.

The results shown in Fig. 2(b) indicate that for $A_x$ from 3.8 to 4, the leading mode is a steady mode with the central symmetry, for $A_x$ from 3.1 to 3.8 the leading mode is oscillatory and only keeps the left-right symmetry, and for $A_x$ from 3 to 3.1, still another leading mode is obtained, which

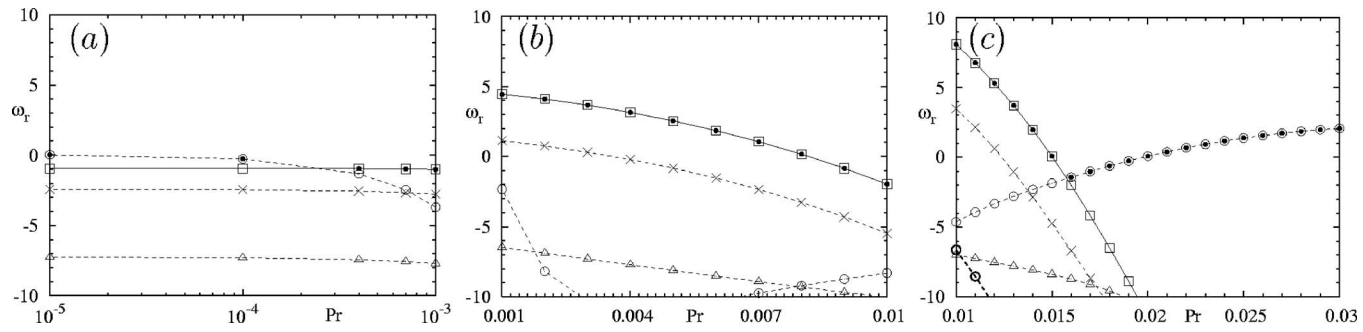


FIG. 4. Real parts $\omega_r$ of the dominant eigenvalues for $0.00001 \leq Pr \leq 0.03$ ($A_x=4$, $A_y=2$): (a) Gr=28 000 for $0.00001 \leq Pr \leq 0.001$, (b) Gr=30 000 for $0.001 \leq Pr \leq 0.01$, and (c) Gr=35 000 for $0.01 \leq Pr \leq 0.03$. Solid curves represent steady modes and dashed curves oscillatory modes. Circles indicate $S_c$ modes, squares $S_l$ modes, triangles $S_r$ modes, and crosses $S$ modes. The black dots indicate the leading mode.

is oscillatory but only keeps the central symmetry. Calculations for other $A_x$ values reveal that the mode obtained for $A_x=3$ remains the leading mode almost down to $A_x=2$ [Fig. 2(a)], and that for $A_x$ between 4 and 5, the leading mode is steady but corresponds alternately to a $S_c$ mode with the central symmetry and a $S_l$ mode with the left-right symmetry [Fig. 2(c)]. The more striking observation is thus the frequent changes of instability modes when $A_x$ is modified. Concerning the angular frequencies of the oscillatory modes, they globally vary between 200 and 50, but for the leading modes, the variation occurs from values around 150 for $A_x=2$ to values around 65 for $A_x=3.7$.

Still for Pr=0.01, the longitudinal aspect ratio is now fixed to $A_x=4$, and the transverse extension is decreased from $A_y=6$ to $A_y=1$. The chosen values of Gr are Gr=23 000 for $4\leq A_y\leq 6$, Gr=26 000 for $3\leq A_y\leq 4$, Gr=30 000 for $2\leq A_y\leq 3$, and Gr=35 000 for $1\leq A_y\leq 2$. The results are shown in Fig. 3. They still indicate very frequent changes of instability modes. For $A_x=4$ and Pr=0.01, the leading mode is found to be steady in a large range of $A_y$, first for $3\leq A_y\leq 6$ [Figs. 3(c) and 3(d)] and also around $A_y=2$ [Figs. 3(a) and 3(b)]. The mode is still either a $S_c$ mode with the central symmetry or a $S_l$ mode with the left-right symmetry. Oscillatory transitions are however expected for $A_y$ between 2.4 and 2.8 [Fig. 3(b)], and for $A_y\leq 1.6$ [Fig. 3(a)], and they correspond to a $S$ mode with all the symmetries and to a $S_r$ mode with the $\pi$-rotational symmetry, respectively. The frequencies of the oscillatory modes extend from values less than ten to values up to 240, but the frequencies of the leading modes are in a smaller range between 160 and 210.

Finally, the effect of the Prandtl number ($0.00001\leq \mathrm{Pr} \leq 0.03$) was studied for a cavity with aspect ratios $A_x=4$ and $A_y=2$. The chosen values of Gr are Gr=35 000 for $0.01\leq \mathrm{Pr}\leq 0.03$, Gr=30 000 for $0.001\leq \mathrm{Pr}\leq 0.01$, and Gr=28 000 for $0.00001\leq \mathrm{Pr}\leq 0.001$. The results are presented in Fig. 4. For $A_x=4$ and $A_y=2$, the leading mode is steady in a large range of Pr values, between 0.001 and 0.015, and it corresponds to a mode with the left-right symmetry. For stronger values of Pr [Fig. 4(c)], the transition is oscillatory with angular frequencies between 80 and 100 and corresponds to a mode with the central symmetry, in agreement with the oscillatory flow found by Henry and Buffat[9] in the same cavity for Pr=0.026. The authors also found an oscillatory transition of the same type but with a longer period in the limit case Pr=0. Our calculations confirm this result, as the leading mode becomes oscillatory when Pr is sufficiently small [Fig. 4(a)], and the angular frequency is really small, around 15 compared to 90 for Pr=0.026. It is also shown that this oscillatory mode is dominant only for very small values of Pr, and is not at all characteristic of the behaviors obtained in the whole domain of small Prandtl numbers corresponding to liquid metals.

For the first time, the different modes involved in the first flow transition in a laterally heated parallelepipedic cavity have been obtained for a wide range of characteristic parameters. It is shown that these modes, which can be characterized by their symmetries, often change when the aspect ratios and Prandtl numbers are modified. The four types of oscillatory modes corresponding to the different possible symmetries of the system can be obtained. Steady modes are, however, the leading modes in different ranges of parameters. In these zones, the oscillatory transition will therefore appear later, on secondary branches of solutions. A last remark concerns the limit case Pr=0, which cannot be considered as representative of the situations at low Prandtl numbers, as the oscillatory mode found for Pr=0 does not remain the leading mode beyond Pr=0.001. The next step of this work will be to develop the direct calculation of the bifurcation points and use it to follow the different thresholds corresponding to these critical modes by continuation.

The calculations were carried out on a NEC-SX5 computer with the support of the CNRS through the "Institut du développement et des ressources en informatique scientifique."

[1] G. Müller and A. Ostrogorsky, "Convection in melt growth," in *Handbook of Crystal Growth: Growth Mechanisms and Dynamics*, Vol. 2b, edited by D. T. J. Hurle (North-Holland, Amsterdam, 1993).
[2] D. T. J. Hurle, "Temperature oscillations in molten metals and their relationship to growth striae in melt-grown crystals," Philos. Mag. **13**, 305 (1966).
[3] D. T. J. Hurle, E. Jakeman, and C. P. Johnson, "Convective temperature oscillations in molten gallium," J. Fluid Mech. **64**, 565 (1974).
[4] J. E. Hart, "Stability of thin non-rotating Hadley circulations," J. Atmos. Sci. **29**, 687 (1972).
[5] P. Laure, "Etude des mouvements de convection dans une cavité rectangulaire soumise à un gradient de température horizontal," J. Mec. Theor. Appl. **6**, 351 (1987).
[6] B. Roux (ed.), "Numerical simulation of oscillatory convection in low-Pr fluids," in *Notes on Numerical Fluid Mechanics* (Vieweg, Wiesbaden, Germany, 1990), Vol. 27.
[7] B. Hof, A. Juel, L. Zhao, D. Henry, H. BenHadid, and T. Mullin, "On the onset of oscillatory convection in molten gallium," J. Fluid Mech. **515**, 391 (2004).
[8] M. Afrid and A. Zebib, "Oscillatory three-dimensional convection in rectangular cavities and enclosures," Phys. Fluids A **2**, 1318 (1990).
[9] D. Henry and M. Buffat, "Two and three-dimensional numerical simulations of the transition to oscillatory convection in low-Prandtl number fluids," J. Fluid Mech. **374**, 145 (1998).
[10] S. Wakitani, "Numerical study of three-dimensional oscillatory natural convection at low Prandtl number in rectangular enclosures," J. Heat Transfer **123**, 77 (2001).
[11] H. BenHadid and D. Henry, "Numerical study of convection in the horizontal Bridgman configuration under the action of a constant magnetic field. Part 2: Three-dimensional flow," J. Fluid Mech. **333**, 57 (1997).
[12] C. K. Mamun and L. S. Tuckerman, "Asymmetry and Hopf bifurcation in spherical Couette flow," Phys. Fluids **7**, 80 (1995).
[13] A. Bergeon, D. Henry, H. BenHadid, and L. S. Tuckerman, "Marangoni convection in binary mixtures with Soret effect," J. Fluid Mech. **375**, 143 (1998).